Petroleum Science 21 (2024) 3157–3165

Contents lists available at ScienceDirect

Petroleum Science

journal homepage: www.keaipublishing.com/en/journals/petroleum-science

Original Paper

Seismic modeling by combining the finite-difference scheme with the numerical dispersion suppression neural network

Hong-Yong Yan [a, b, *]

[a] Key Laboratory of Petroleum Resources Research, Institute of Geology and Geophysics, Chinese Academy of Sciences, Beijing, 100029, China
[b] Innovation Academy for Earth Science, Chinese Academy of Sciences, Beijing, 100029, China

ARTICLE INFO

Article history:
Received 16 December 2023
Received in revised form
27 March 2024
Accepted 23 June 2024
Available online 25 June 2024

Edited by Meng-Jiao Zhou

Keywords:
Finite difference
Seismic modeling
Numerical dispersion suppression
Computational accuracy
Computational efficiency

ABSTRACT

Seismic finite-difference (FD) modeling suffers from numerical dispersion including both the temporal and spatial dispersion, which can decrease the accuracy of the numerical modeling. To improve the accuracy and efficiency of the conventional numerical modeling, I develop a new seismic modeling method by combining the FD scheme with the numerical dispersion suppression neural network (NDSNN). This method involves the following steps. First, a training data set composed of a small number of wavefield snapshots is generated. The wavefield snapshots with the low-accuracy wavefield data and the high-accuracy wavefield data are paired, and the low-accuracy wavefield snapshots involve the obvious numerical dispersion including both the temporal and spatial dispersion. Second, the NDSNN is trained until the network converges to simultaneously suppress the temporal and spatial dispersion. Third, the entire set of low-accuracy wavefield data is computed quickly using FD modeling with the large time step and the coarse grid. Fourth, the NDSNN is applied to the entire set of low-accuracy wavefield data to suppress the numerical dispersion including the temporal and spatial dispersion. Numerical modeling examples verify the effectiveness of my proposed method in improving the computational accuracy and efficiency.

1. Introduction

Finite-difference (FD) methods have been widely used to perform seismic modeling for their easy implementation and small computational costs (Kelly et al., 1976; Virieux, 1984; Robertsson et al., 1994; Moczo et al., 2000; Yang et al., 2012; Yao et al., 2016; Liu, 2020). However, seismic FD modeling suffers from numerical dispersion including both the temporal and spatial dispersion, which can decrease the accuracy of the numerical modeling. To obtain accurate seismic waveforms, small time steps, fine grids and high-order FD approximations are often adopted to suppress the numerical dispersion. However, these approaches significantly increase the computational cost and memory usage (Li et al., 2016). The seismic FD modeling has always been confronted with the challenges of the temporal and spatial dispersion suppression (Liu, 2020).

Methods to suppress numerical dispersion have been widely studied. There are two major kinds of methods to suppress temporal dispersion. The first is the time-space domain dispersion-based FD method, which determines the spatial FD coefficients by using the Taylor series expansion of time-space domain dispersion relation (Finkelstein and Kastner, 2007; Liu and Sen, 2009a; Ren and Liu, 2015; Ren and Li, 2017). The second is the filtering-based method, which proposes that the temporal dispersion can be filtered after propagation (Stork, 2013; Dai et al., 2014; Wang and Xu, 2015; Li et al., 2016). To suppress spatial dispersion, two main kinds of methods have been developed. The first is the implicit spatial FD method. This method calculates the spatial derivative value by combining the spatial derivatives of each point with the spatial derivatives of adjacent points (Lele, 1992; Liu and Sen, 2009b; Kosloff et al., 2010; Chu and Stoffa, 2012). The second is the optimal spatial FD method. This method computes the spatial FD coefficients by using optimal algorithms (Liu, 2013; Zhang and Yao, 2013; Yan et al., 2016; Yang et al., 2017).

In recent years, artificial intelligence technologies have emerged

* Corresponding Author. Key Laboratory of Petroleum Resources Research, Institute of Geology and Geophysics, Chinese Academy of Sciences, Beijing, 100029, China.
E-mail address: yanhongyong@mail.iggcas.ac.cn.

https://doi.org/10.1016/j.petsci.2024.06.014

for geophysical applications. Using machine learning, especially deep learning, to suppress numerical dispersion for seismic FD modeling has also attracted attention from the academic circle. Siahkoohi et al. (2018, 2019a, 2019b) applied the deep convolutional neural networks and the transfer learning to mitigating the numerical dispersion from wave simulations. Kaur et al. (2019) suggested using generative adversarial networks to overcome the spatial dispersion of FD extrapolation. Zhang et al. (2022) proposed using deep convolutional neural networks to extract wavefield features for the spatial dispersion correction. Han et al. (2022) employed convolutional and recurrent neural networks with semi-supervised learning to eliminate time dispersion caused by seismic modeling. Gadylshin et al. (2022, 2023) adopted deep neural networks in the time domain and the frequency domain successively to mitigate the spatial dispersion of seismic data. Xu et al. (2023) put forward a pix2pix network to remove the temporal dispersion from elastic FD modeling. However, in the training data set of this neural network, the low accuracy of the raw data and the high accuracy of the target data are only related to whether there is obvious temporal dispersion, so the neural network can only remove the temporal dispersion. Yan and Xu (2024) proposed an improved pix2pix algorithm to stably and efficiently suppress the spatial dispersion of seismic FD modeling. These methods can suppress the temporal dispersion or the spatial dispersion, but none of them is used to simultaneously suppress the temporal and spatial dispersion.

In this paper, I propose a new seismic modeling method by combining the FD scheme with the numerical dispersion suppression neural network (NDSNN). The NDSNN is constructed based on the idea of the stable image-to-image translation, and it can be used to suppress the numerical dispersion including both the temporal and spatial dispersion from seismic FD modeling. Numerical experiments for a homogeneous model and a heterogeneous model verify the effectiveness of my proposed method in suppressing the numerical dispersion and saving computing costs.

2. Theory and method

The acoustic wave equation is often used to approximate the propagation of seismic waves. The 2D acoustic wave equation is

$$\frac{1}{v^2}\frac{\partial^2 p}{\partial t^2}=\frac{\partial^2 p}{\partial x^2}+\frac{\partial^2 p}{\partial z^2}, \tag{1}$$

where v is the velocity and $p = p\,(x, z, t)$ is the scalar wavefield.

The FD methods are often applied to solve the acoustic wave equation. A 2nd-order FD is usually used for approximating temporal derivatives:

$$\frac{\partial^2 p}{\partial t^2}\approx\frac{1}{\tau^2}\left[-2p^0_{0,0}+\left(p^{-1}_{0,0}+p^1_{0,0}\right)\right], \tag{2}$$

where τ is the time step, $p^n_{m,j}=p(x+mh,z+jh,t+n\tau)$, and h is the grid size.

Generally, a $(2M)$th-order FD is used for spatial derivatives:

$$\frac{\partial^2 p}{\partial x^2}\approx\frac{1}{h^2}\left[a_0p^0_{0,0}+\sum_{m=1}^{M}a_m\left(p^0_{-m,0}+p^0_{m,0}\right)\right], \tag{3a}$$

$$\frac{\partial^2 p}{\partial z^2}\approx\frac{1}{h^2}\left[a_0p^0_{0,0}+\sum_{m=1}^{M}a_m\left(p^0_{0,-m}+p^0_{0,m}\right)\right], \tag{3b}$$

where a_m are FD coefficients.

However, as the FD methods replace derivatives with difference approximations in solving wave equation, it's inevitable that seismic FD modeling suffers from the numerical dispersion including the temporal and spatial dispersion. Especially when the large time step and the coarse grid are used, the numerical dispersion can be very severe. Small time steps and fine grids may improve the seismic FD modeling accuracy but will significantly increase the memory usage and computational cost. Fig. 1 shows the snapshots of acoustic FD modeling for different time steps and grid sizes. From Fig. 1, it can be seen that the severe numerical dispersion is diminished at small time step and grid size.

To realize the high-accuracy and high-efficiency seismic FD modeling, a stable approach that combines the pix2pix algorithm (Isola et al., 2017) with the Sobel operator (Sobel and Feldman, 1968) is proposed to construct the NDSNN. The pix2pix algorithm (Isola et al., 2017) is a generative adversarial network (GAN) framework for the image-to-image translation, which draws on the idea of introducing additional conditional information of the conditional generative adversarial nets. The pix2pix algorithm requires the input of one-to-one matched paired data: The raw data and the target data. The raw data is used as the input of the generator. Besides, the raw data is also used as the input of the discriminator along with the target data or the data generated by the generator, and then trained to ultimately achieve the function of converting one type of data to the other. The algorithm not only learns the mapping from the input image to the output image, but also learns the loss function to train the mapping, making it highly versatile (Isola et al., 2017).

The loss function of the pix2pix algorithm is defined as (Isola et al., 2017)

$$\mathscr{L}_{\text{pix2pix}}(G,D)=\arg\min_{G}\max_{D}\left\{\mathscr{L}_{\text{cGAN}}(G,D)+\lambda_{\text{L}_1}\mathscr{L}_{\text{L}_1}(G)\right\}, \tag{4}$$

where

$$\mathscr{L}_{\text{cGAN}}(G,D)=E_{y_\text{r},y_\text{t}}[\log(D(y_\text{r},y_\text{t}))]+E_{y_\text{r}}[\log(1-D(y_\text{r},G(y_\text{r}))], \tag{5a}$$

$$\mathscr{L}_{\text{L}_1}(G)=E_{y_\text{r},y_\text{t}}\left[\|y_\text{t}-G(y_\text{r})\|_1\right], \tag{5b}$$

G is the generator, D is the discriminator, λ_{L_1} is the certainty coefficient of the L_1-norm loss term, E is the mean operator, y_r is the raw data, and y_t is the target data.

This algorithm undergoes continuous iterative training, and when the entire network converges, the generator can achieve the function of mapping from the raw data to the target data. In this process, the pix2pix algorithm uses L_1 norm to restrict the generator, but the training result of the algorithm is unstable and the quality of generated images is unsatisfactory (Wang et al., 2018). To improve the stability of the conventional pix2pix algorithm (Isola et al., 2017), the Sobel operator (Sobel and Feldman, 1968) is applied in seismic wavefield data processing (Yan and Xu, 2024).

The Sobel operator (Sobel and Feldman, 1968) is an important processing method in the field of computer vision, mainly used to obtain the first-order gradient value of a digital image, and is usually used for edge detection. The Sobel operator uses two 3×3 matrix operators to convolution with the original image to obtain horizontal and vertical gradient values, respectively. Then, the gradient values in these two directions are combined to obtain the total gradient value. If the total gradient value is greater than a certain threshold, the point is considered an edge point. The horizontal and vertical operators of the Sobel operator are as follows (Sobel and Feldman, 1968):

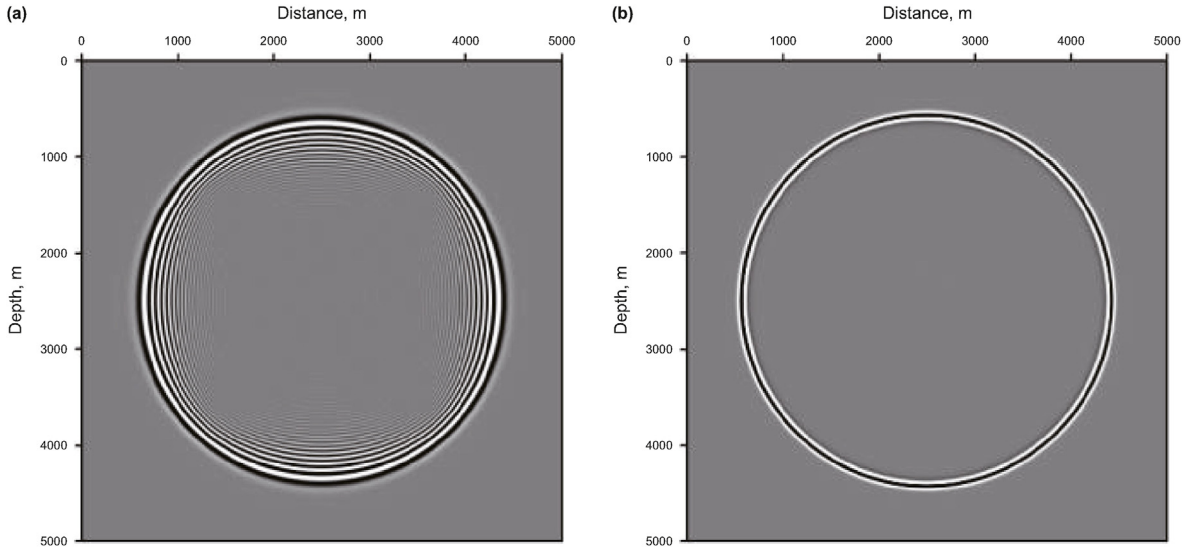

Fig. 1. Snapshots at $t = 1.0$ s of acoustic FD modeling for the homogeneous model. The model size is 5000 m × 5000 m. The source is located in the model center. The P-wave velocity is 2000 m/s. A Ricker wavelet with a main frequency of 25 Hz is used to generate vibrations. The 2nd-order temporal FD and the 2nd-order spatial FD are used to solve the acoustic wave equation for seismic modeling. **(a)** Low-accuracy snapshot generated with $\tau = 0.002$ s and $h = 20$ m. **(b)** High-accuracy snapshot generated with $\tau = 0.0005$ s and $h = 5$ m.

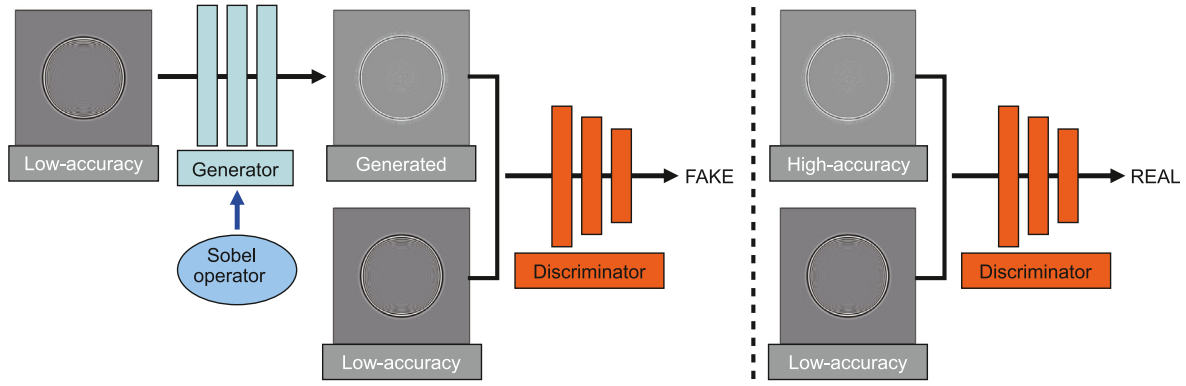

Fig. 2. The training procedure of the NDSSN.

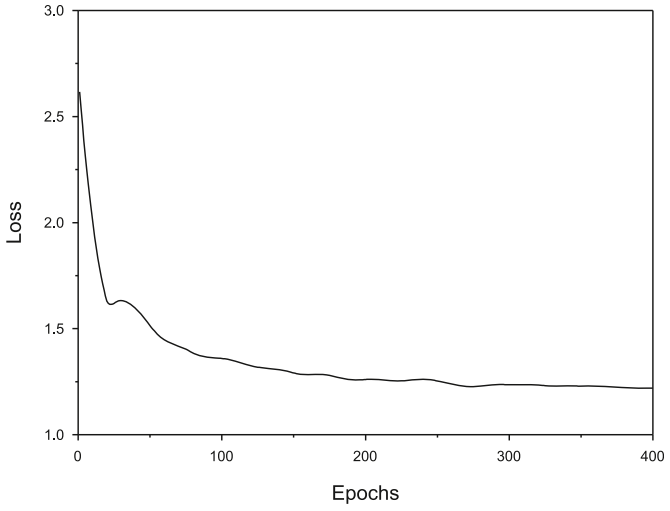

Fig. 3. Training losses of epochs for the homogeneous model.

$$\boldsymbol{S_x} = \begin{bmatrix} -1 & 0 & 1 \\ -2 & 0 & 2 \\ -1 & 0 & 1 \end{bmatrix}, \tag{6a}$$

$$\boldsymbol{S_z} = \begin{bmatrix} 1 & 2 & 1 \\ 0 & 0 & 0 \\ -1 & -2 & -1 \end{bmatrix}. \tag{6b}$$

The Sobel operator is use to process image, and the calculation formula is as follow (Sobel and Feldman, 1968):

$$S = \sqrt{(\boldsymbol{S_x} * \boldsymbol{A})^2 + (\boldsymbol{S_z} * \boldsymbol{A})^2}, \tag{7}$$

where $\boldsymbol{A}$ is the input data, S is the total gradient value, and $*$ is the convolution operation.

By combining the pix2pix algorithm (Isola et al., 2017) with the Sobel operator (Sobel and Feldman, 1968), the loss function of the NDSNN is defined as

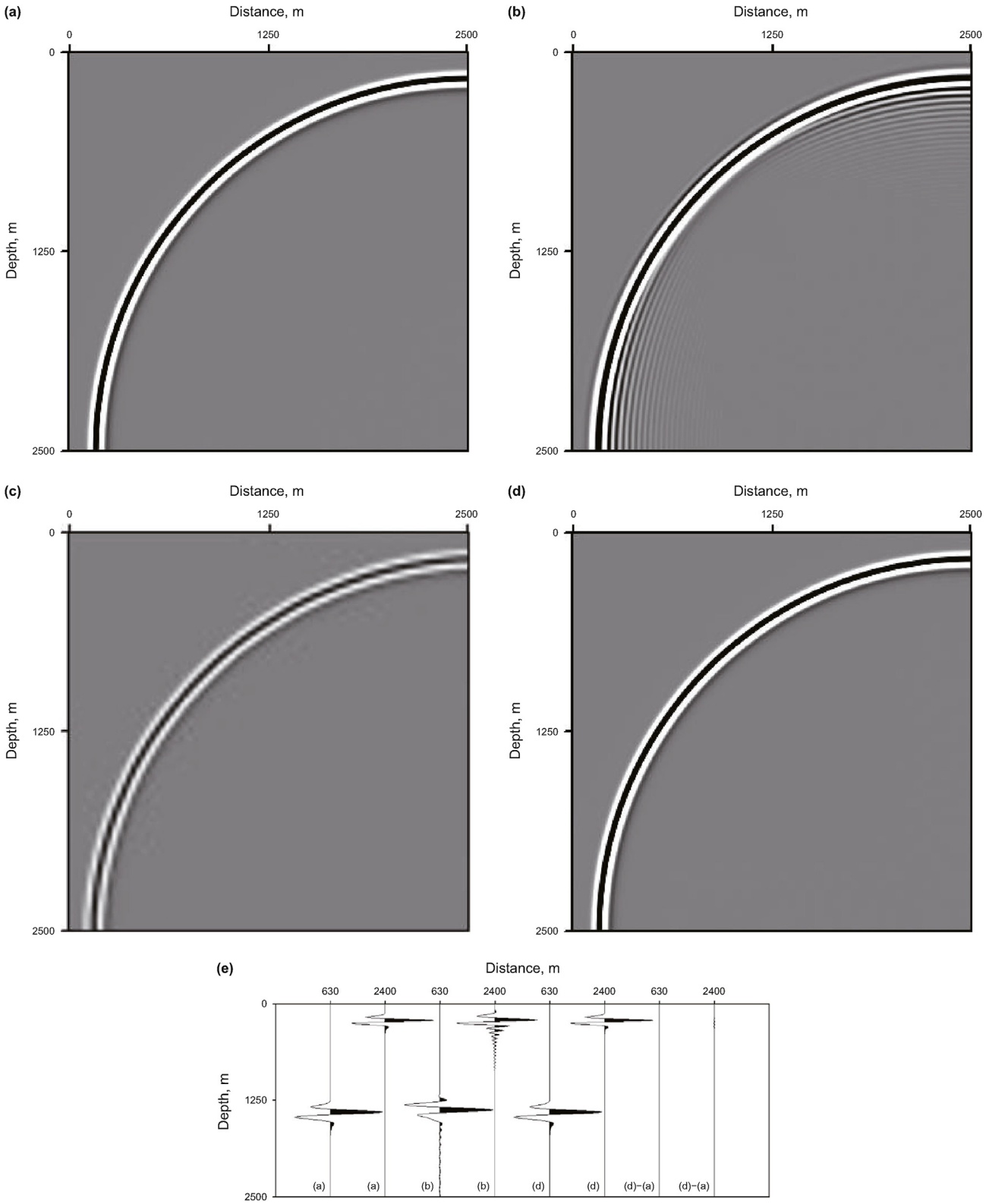

Fig. 4. Snapshots at $t = 1.2$ s and their differences of acoustic FD modeling for the homogeneous model. The source is located at (2500 m, 2500 m). **(a)** High-accuracy snapshot generated with $\tau = 0.0005$ s and $h = 5$ m. **(b)** Low-accuracy snapshot generated with $\tau = 0.002$ s and $h = 10$ m. **(c)** Snapshot (b) after dispersion correction by the conventional pix2pix algorithm without the Sobel operator. **(d)** Snapshot (b) after dispersion correction by the NDSNN. **(e)** Some traces from (a), (b), (d), and the differences between (d) and (a).

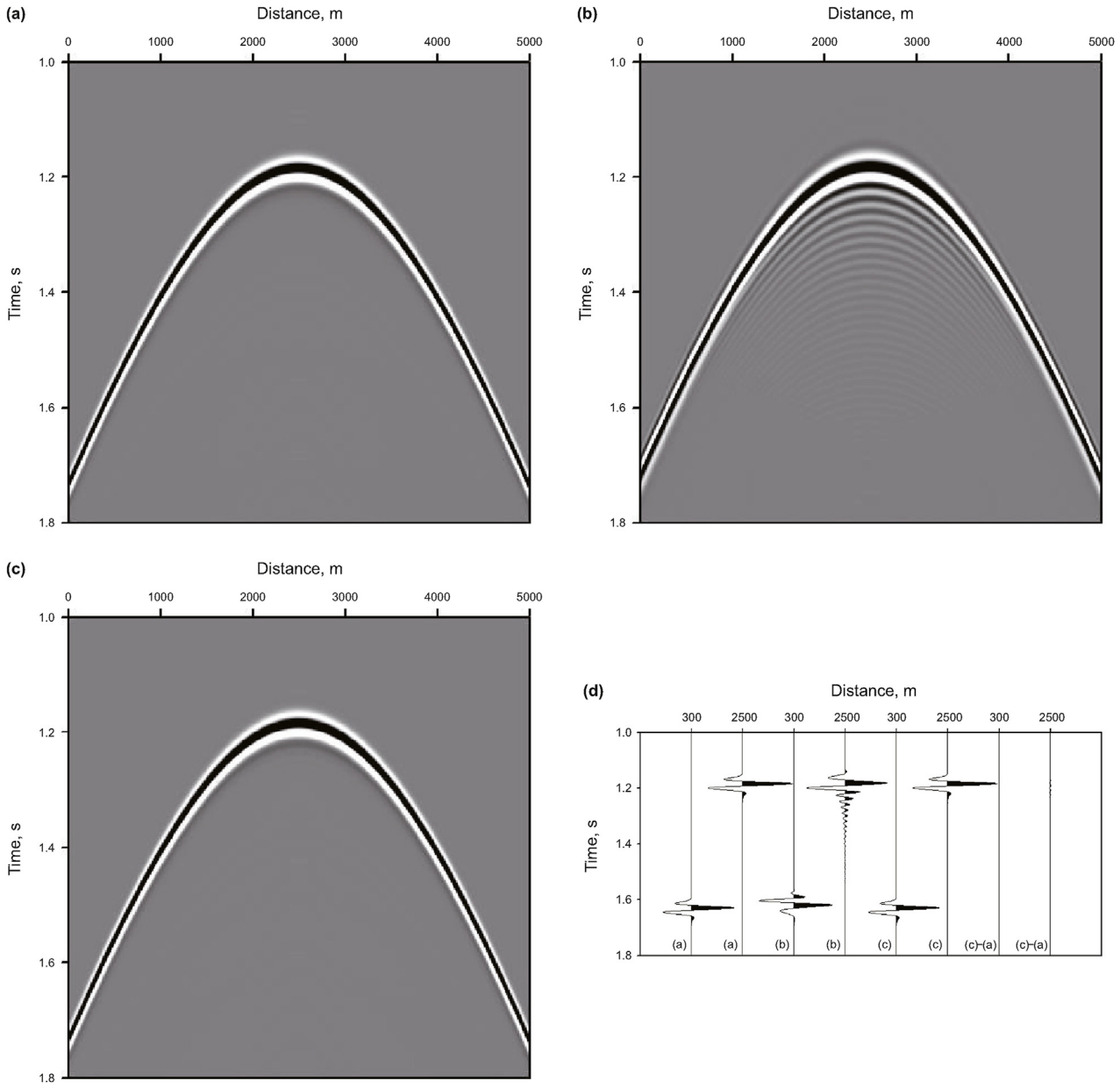

Fig. 5. Shot records and their differences of acoustic FD modeling for the homogeneous model. The source is located at (2500 m, 2500 m). The depth of the receivers is 200 m. **(a)** High-accuracy shot record generated with $\tau = 0.0005$ s and $h = 5$ m. **(b)** Low-accuracy shot record generated with $\tau = 0.002$ s and $h = 10$ m. **(c)** Corrected shot record by the NDSNN. **(d)** Some traces from (a), (b), (c) and the differences between (c) and (a).

$$\mathscr{L}(G,D) = \arg\min_{G}\max_{D}\left\{\mathscr{L}_{\mathrm{cGAN}}(G,D) + \lambda_{\mathrm{L}_1}\mathscr{L}_{\mathrm{L}_1}(G) + \lambda_{\mathrm{S}}\mathscr{L}_{\mathrm{S}}(G)\right\}, \tag{8}$$

where

$$\mathscr{L}_{\mathrm{S}}(G) = E_{y_{\mathrm{r}},y_{\mathrm{t}}}\left[\|S(y_{\mathrm{t}}) - S(G(y_{\mathrm{r}}))\|_1\right], \tag{9}$$

and λ_{S} is the certainty coefficient of the Sobel operator loss term.

The NDSNN based on the stable pix2pix algorithm (Yan and Xu, 2024) consists of a generator and a discriminator. It adopts an encoder-decoder network (Hinton and Salakhutdinov, 2006) as the generator and a patch-based fully convolutional network (Long et al., 2017) as the discriminator. The generator based on the encoder-decoder network involves five types of modules, namely the initialization module, the encoding module, the residual module, the decoding module and the recovery module. The

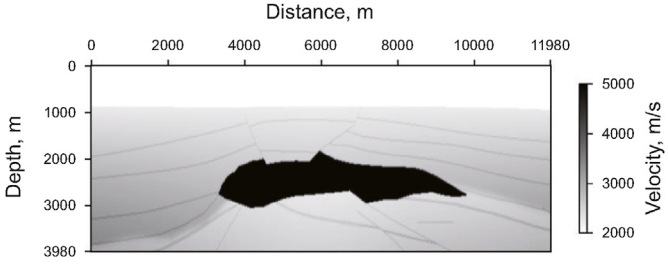

Fig. 6. The velocity model for the modified SEG/EAGE salt model.

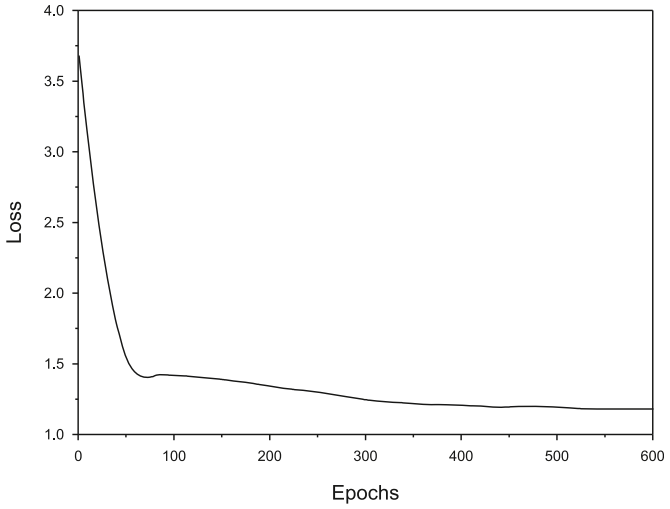

Fig. 7. Training losses of epochs for the modified SEG/EAGE salt model.

discriminator based on the patch-based fully convolutional network is to first split the input data into several small blocks, then make cognitive judgments on each small block, and finally consider the judgment results of all small blocks comprehensively to provide a selection of data sources. The layer number of the discriminator is an important parameter that affects the variation of the loss function value. The basis for selecting this parameter is to make the loss function value change and the network training stable. In addition, in the subsequent numerical experiments, the batch size and the optimizer recommended by Isola et al. (2017) are used.

The basic steps for suppressing the numerical dispersion of seismic FD modeling are as follows: First, a training data set composed of a small number of wavefield snapshots is generated. The wavefield snapshots included the low-accuracy wavefield data (with the obvious numerical dispersion) and the high-accuracy wavefield data (with almost no numerical dispersion) are paired, which matched according to the corresponding time. Here, the low-accuracy wavefield snapshots are seriously polluted by both the temporal and spatial dispersion. The low-accuracy wavefield snapshots and the high-accuracy wavefield snapshots are used as the raw data and the target data respectively. Second, the NDSNN is trained until the network converges to simultaneously suppress the temporal and spatial dispersion. The training procedure of the NDSNN is shown in Fig. 2. The converged generator is used as an operator to suppress numerical dispersion, and the entire set of low-accuracy wavefield data is processed, thus converting the low-accuracy wavefield into the high-accuracy wavefield.

3. Numerical experiments

I apply my method to perform seismic modeling in two examples. The NDSNN is used to suppress the numerical dispersion of the 2D acoustic FD modeling. Here, the 2nd-order temporal FD and the 4th-order spatial FD are used to solve the acoustic wave equation for seismic modeling. In addition, the perfectly matched layer absorbing boundary condition (Bérenger, 1994) is adopted to reduce boundary reflections of the model. The training data sets consist of a small number of the high-accuracy wavefield and the low-accuracy wavefield. The high-accuracy wavefield sets are generated using the small time step and the fine gird, thus almost free from the numerical dispersion. The low-accuracy wavefield sets are generated using the large time step and the coarse gird. In the numerical experiments, every training data set is selected from the simulated wavefield data at the three different seismic sources positions, at each of which randomly involves 100 pairs of high-accuracy and low-accuracy wavefield snapshots. The training data sets are used to train the NDSNN. The entire raw low-accuracy wavefield data sets with dispersion artifacts computed by FD method are applied to test the NDSNN. These two examples are performed to illustrate the effectiveness of the proposed method to

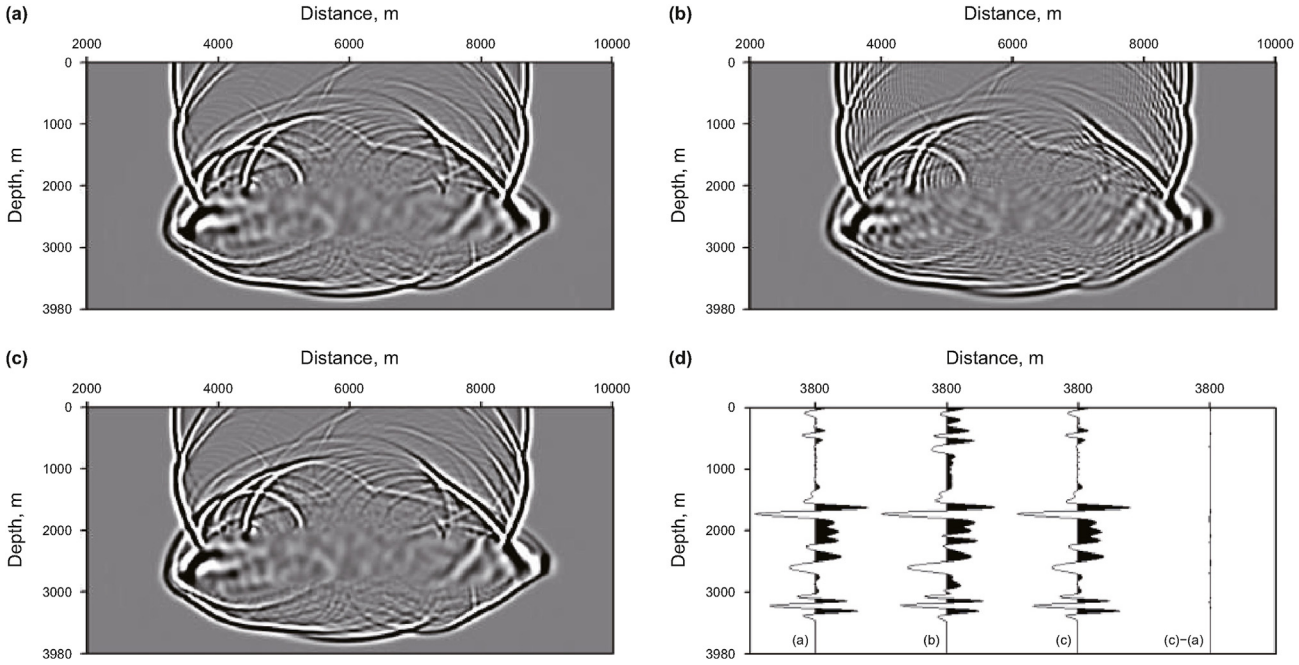

Fig. 8. Snapshots at $t = 1.4$ s and their difference of acoustic FD modeling for the modified SEG/EAGE salt model. The source is located at (6000 m, 220 m). **(a)** High-accuracy snapshot generated with $\tau = 0.0005$ s and $h = 5$ m. **(b)** Low-accuracy snapshot generated with $\tau = 0.002$ s and $h = 20$ m. **(c)** Snapshot (b) after dispersion correction by the NDSNN. **(d)** Some traces from (a), (b) and (c), and the difference between (c) and (a).

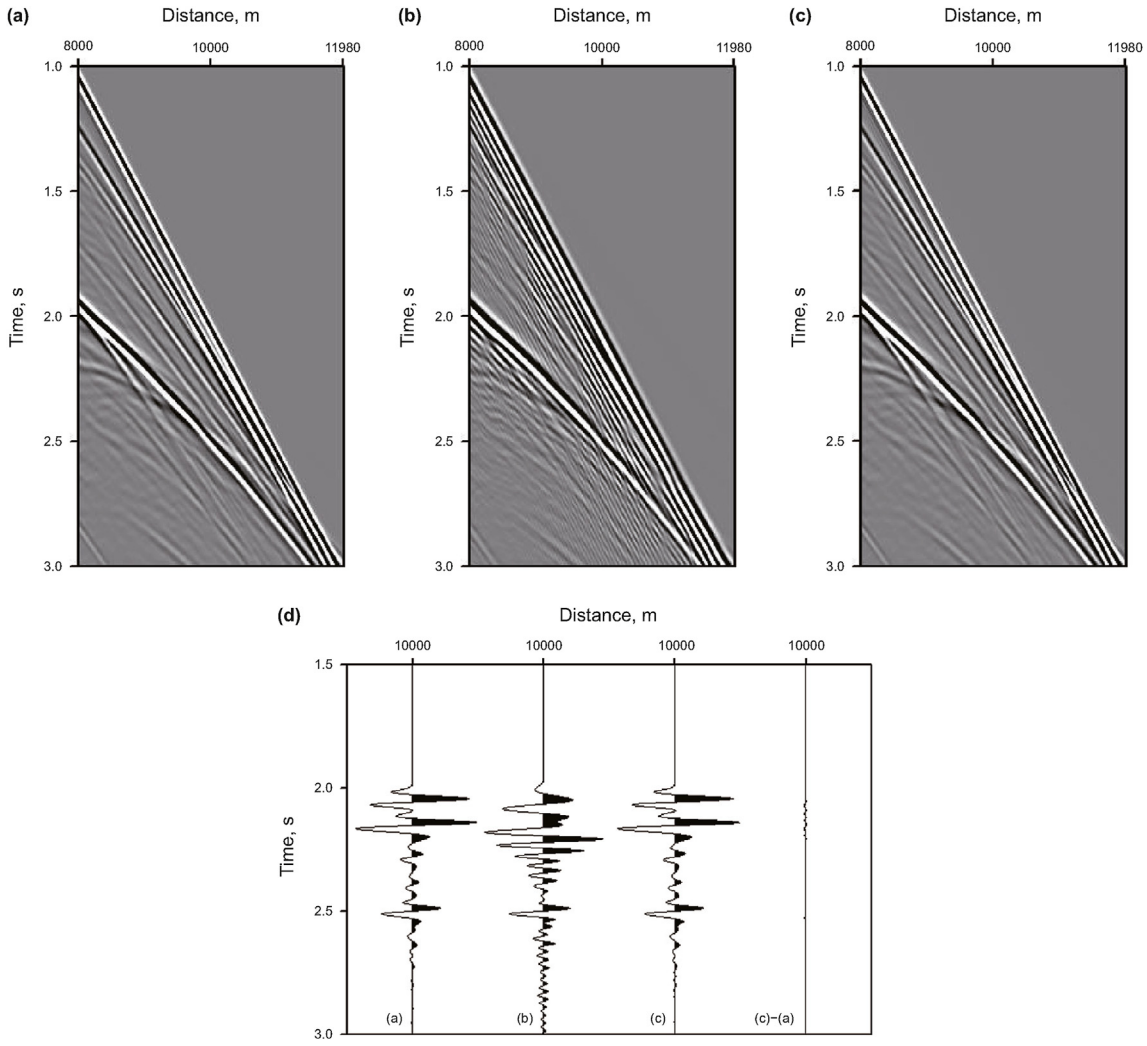

Fig. 9. Shot records and their difference of acoustic FD modeling for the modified SEG/EAGE salt model. The source is located at (6000 m, 220 m). The depth of the receivers is 200 m. **(a)** High-accuracy shot record generated with $\tau = 0.0005$ s and $h = 5$ m. **(b)** Low-accuracy shot record generated with $\tau = 0.002$ s and $h = 20$ m. **(c)** Corrected shot record by the NDSNN. **(d)** Some traces from (a), (b) and (c), and the difference between (c) and (a).

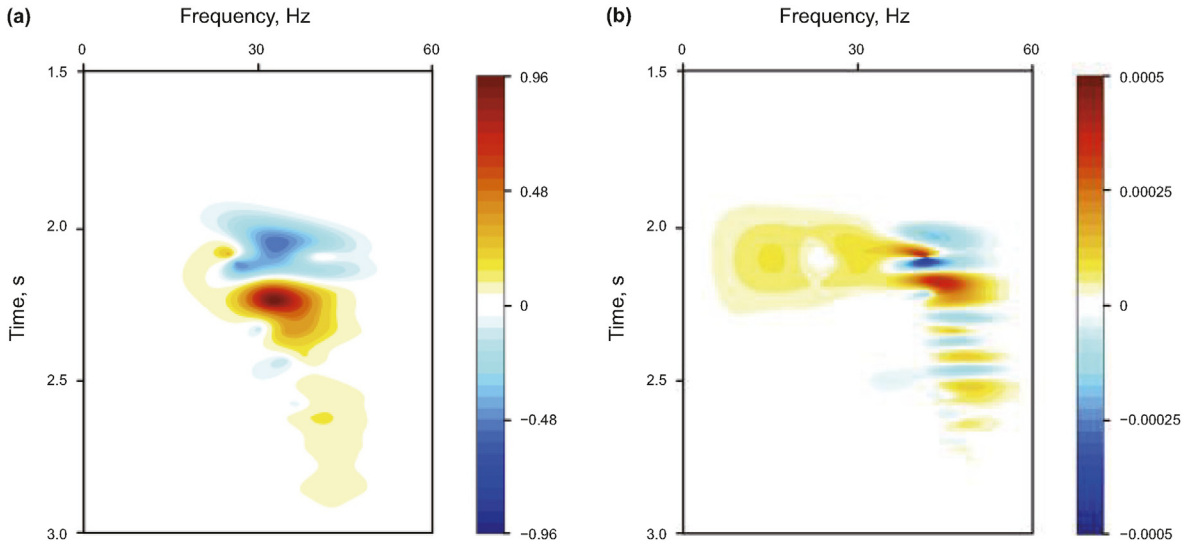

Fig. 10. Globally normalized time-frequency envelope misfits. Here, the formula used for computing misfit comes from Kristeková et al. (2009). **(a)** The misfits between the low-accuracy waveform shown in Fig. 9(b) and high-accuracy waveform shown in Fig. 9(a). **(b)** The misfits between the corrected waveform shown in Fig. 9(c) and high-accuracy waveform shown in Fig. 9(a).

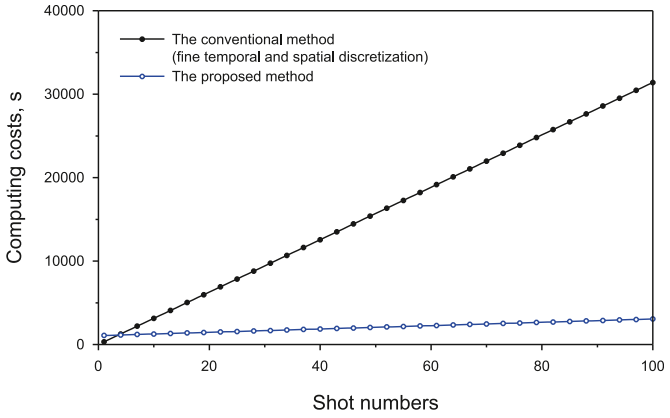

Fig. 11. The computing costs of the different methods for the modified SEG/EAGE salt model.

improve the accuracy and efficiency of seismic FD modeling.

The first example is for a homogeneous model. The size of the model is 5000 m × 5000 m, and the P-wave velocity is 2000 m/s. A Ricker wavelet with a main frequency of 25 Hz is used to generate vibrations. The entire original low-accuracy wavefield data set with dispersion artifacts is computed by FD method with $\tau = 0.002$ s and $h = 10$ m. The generator neural network adopts a nineteen-layer encoder-decoder structure. It involves an initialization module, three encoding modules, eleven residual modules, three decoding modules and a recovery module, in which the encoding modules and decoding modules are connected by the residual modules. The discriminator neural network adopts a five-layer convolutional structure. The certainty coefficients of the L_1-norm loss term and the Sobel operator loss term are 30 and 10 respectively. The batch size is set to 1. The learning rate is set as 0.001. Fig. 3 shows the training losses of epochs for the homogeneous model. As the epoch increases, the loss value gradually stabilizes. The network training is very stable when the epoch reaches 400. The training iteration is taken as 400.

Figs. 4 and 5 display snapshots, shot records and their differences for the homogeneous model. The snapshot and the shot record generated with $\tau = 0.0005$ s and $h = 5$ m have little dispersion and high accuracy. However, the numerical dispersion including both the temporal and spatial dispersion is very obvious in the snapshot and the shot record generated with $\tau = 0.002$ s and $h = 10$ m. From these figures, it can be found that the wavefield after dispersion correction by the NDSNN is very clear and close to the high-accuracy wavefield generated using the small time step and the fine gird. However, from the corrected snapshot by the conventional pix2pix algorithm without the Sobel operator, it can be seen that the numerical dispersion is suppressed but the wavefield is fuzzy. These figures show that the proposed method can steadily and effectively suppress the numerical dispersion including both the temporal and spatial dispersion from seismic FD modeling.

To make a quantitative analysis on the accuracy of the corrected wavefield data sets by the NDSNN, I compute the correlation between the corrected and high-accuracy wavefield data for the homogeneous model. I calculate the Pearson correlation coefficient between two sets of corresponding wavefield data and repeat this procedure over the entire data sets. The average correlation coefficient between the corrected and high-accuracy seismic traces is approximately 0.9988. This further indicates that the wavefield after dispersion correction by the NDSNN is quite close to the high-accuracy wavefield generated using the small time step and the fine gird.

The second example is for a heterogeneous model. Fig. 6 shows the velocity model for the modified Society of Exploration Geophysicists/European Association of Geoscientists and Engineers (SEG/EAGE) salt model. The source is a Ricker wavelet with a main frequency of 16 Hz. The entire original low-accuracy wavefield data set with dispersion artifacts is computed by FD method with $\tau = 0.002$ s and $h = 20$ m. The corresponding training losses are shown in Fig. 7. When the epoch reaches 600, the network training can be extremely stable. The other training parameters and the architecture of the generator and discriminator in the neural network are the same as in the first example.

Figs. 8 and 9 show snapshots, records and their differences for the modified SEG/EAGE salt model. Figs. 8(b) and 9(b) display that there are visible dispersion artifacts in the low-accuracy snapshot and record. Fig. 8(c) and (a) suggest that the corrected snapshot by the NDSNN is quite close to the high-accuracy snapshot, and their difference shown in Fig. 8(d) is very small. Fig. 9 displays the similar results. From Figs. 8 and 9, we can see that the proposed method has great accuracy and it effectively suppresses the numerical dispersion of seismic FD modeling.

To quantify the accuracy of the corrected wavefield by the NDSNN, I use the globally normalized time-frequency envelope misfit criteria (Kristeková et al., 2009) to characterize the difference between two waveforms for the modified SEG/EAGE salt model. Fig. 10 shows the globally normalized time-frequency envelope misfits between the low-accuracy and high-accuracy waveforms and the corrected and high-accuracy waveforms. It is evident that the corrected waveform exhibits much smaller misfit than the raw low-accuracy waveform. The quantitative analysis demonstrates that the NDSNN decreases significantly the misfits between the seismic waveforms by suppressing the numerical dispersion.

Finally, I discuss the computational efficiency of the proposed method. The total computing cost of the proposed method involves the generating time of the training data set, the NDSNN training time, the computing time for simulating the entire low-accuracy wavefield data set using the large time step and the coarse grid, and the time for using the NDSNN to process the entire low-accuracy wavefield data set. Fig. 11 shows the computing costs of the proposed method and the conventional method for the modified SEG/EAGE salt model. The computations of the different methods are performed on the same computer (ThinkPad with Intel Core i7-9850H CPU and 16 GB memory). For these two methods, the computing time increases with the increase of the shot number, especially the soaring computing cost of the conventional method, as the modeling uses the fine temporal and spatial discretization. For my proposed method, even with a small number of shots that need to be corrected, it also costs time in generating training set, training neural network, and correcting wavefield. Therefore, when the proposed method is used to simulate a small number of shots, it may not have advantage in computational efficiency compared to the conventional FD method with the small time step and the fine grid. However, as is shown in Fig. 11, when the shot number of seismic modeling exceeds 3, my proposed method starts to show obvious advantages in saving computing costs without compromising accuracy.

4. Conclusions

I have presented a new method to improve seismic modeling performance by combining the FD scheme with the NDSNN. The NDSNN is used to simultaneously suppress the temporal and spatial dispersion of seismic FD modeling. Numerical modeling examples indicate that the proposed method can effectively improve the accuracy of seismic FD modeling. For large geologic models or large-scale seismic numerical modeling, the proposed method can

greatly reduce the computational cost with necessary accuracy. Moreover, the larger the model or the scale is, the more obvious the advantage of the proposed method can be found. Because the numerical dispersion is independent of the particular mathematical model, the proposed method can be extended directly to 3D seismic wave equation modeling, inversion and migration. However, in 3D, the amount of data and the application time may increase significantly. In addition, the retraining of the NDSNN is required each time the geologic model is changed, which restricts the applicability of the proposed method because training is time consuming. Thus, the future development trends of this method could be the generalization of the network and the application of the deep learning approaches that require less training.

CRediT authorship contribution statement

Hong-Yong Yan: Writing – review & editing, Writing – original draft, Visualization, Validation, Supervision, Software, Resources, Project administration, Methodology, Investigation, Funding acquisition, Formal analysis, Data curation, Conceptualization.

Declaration of competing interest

The authors declare that they have no known competing financial interests or personal relationships that could have appeared to influence the work reported in this paper.

Acknowledgements

This work was supported by the National Natural Science Foundation of China (grant numbers: 41874160 and 92055213).

References

Bérenger, J.P., 1994. A perfectly matched layer for the absorption of electromagnetic waves. J. Comput. Phys. 114, 185–200. https://doi.org/10.1006/jcph.1994.1159.
Chu, C., Stoffa, P.L., 2012. Implicit finite-difference simulations of seismic wave propagation. Geophysics 77 (2), T57–T67. https://doi.org/10.1190/GEO2011-0180.1.
Dai, N., Liu, H., Wu, W., 2014. Solutions to numerical dispersion error of time FD in RTM. In: 84th Annual International Meeting, SEG, Expanded Abstracts, pp. 4027–4031. https://doi.org/10.1190/segam2014-0858.1.
Finkelstein, B., Kastner, R., 2007. Finite difference time domain dispersion reduction schemes. J. Comput. Phys. 221, 422–438. https://doi.org/10.1016/j.jcp.2006.06.016.
Gadylshin, K., Lisitsa, V., Gadylshina, K., et al., 2023. Frequency domain numerical dispersion mitigation network. In: International Conference on Computational Science and its Applications, pp. 31–44. https://doi.org/10.1007/978-3-031-37111-0_3.
Gadylshin, K., Vishnevsky, D., Gadylshina, K., et al., 2022. Numerical dispersion mitigation neural network for seismic modeling. Geophysics 87 (3), T237–T249. https://doi.org/10.1190/GEO2021-0242.1.
Han, Y., Wu, B., Yao, G., et al., 2022. Eliminate time dispersion of seismic wavefield simulation with semi-supervised deep learning. Energies 15, 7701. https://doi.org/10.3390/en15207701.
Hinton, G.E., Salakhutdinov, R.R., 2006. Reducing the dimensionality of data with neural networks. Science 313 (5786), 504–507. https://doi.org/10.1126/science.1127647.
Isola, P., Zhu, J., Zhou, T., et al., 2017. Image-to-image translation with conditional adversarial networks. In: IEEE Conference on Computer Vision and Pattern Recognition, pp. 5967–5976. https://doi.org/10.1109/CVPR.2017.632.
Kaur, H., Fomel, S., Pham, N., 2019. Overcoming numerical dispersion of finite-difference wave extrapolation using deep learning. In: 89th Annual International Meeting. SEG, Expanded Abstracts, pp. 2318–2322 doi:10.1190/segam2019-3207486.1.
Kelly, K.R., Ward, R., Treitel, W.S., et al., 1976. Synthetic seismograms: a finite-difference approach. Geophysics 41, 2–27. https://doi.org/10.1190/1.1440605.
Kosloff, D., Pestana, R.C., Tal-Ezer, H., 2010. Acoustic and elastic numerical wave simulations by recursive spatial derivative operators. Geophysics 75 (6), T167–T174. https://doi.org/10.1190/1.3485217.
Kristeková, M., Kristek, J., Moczo, P., 2009. Time-frequency misfit and goodness-of-fit criteria for quantitative comparison of time signals. Geophys. J. Int. 178, 813–825. https://doi:10.1111/j.1365-246X.2009.04177.x.
Lele, S.K., 1992. Compact finite difference schemes with spectral-like resolution. J. Comput. Phys. 103, 16–42. https://doi.org/10.1016/0021-9991(92)90324-R.
Li, Y.E., Wong, M., Clapp, R., 2016. Equivalent accuracy at a fraction of the cost: Overcoming temporal dispersion. Geophysics 81 (5), T189–T196. https://doi.org/10.1190/GEO2015-0398.1.
Liu, Y., 2013. Globally optimal finite-difference schemes based on least squares. Geophysics 78 (4), T113–T132. https://doi.org/10.1190/GEO2012-0480.1.
Liu, Y., 2020. Acoustic and elastic finite-difference modeling by optimal variable-length spatial operators. Geophysics 85 (2), T57–T70. https://doi.org/10.1190/GEO2019-0145.1.
Liu, Y., Sen, M.K., 2009a. A new time-space domain high-order finite-difference method for the acoustic wave equation. J. Comput. Phys. 228, 8779–8806. https://doi.org/10.1016/j.jcp.2009.08.027.
Liu, Y., Sen, M.K., 2009b. An implicit staggered-grid finite-difference method for seismic modeling. Geophys. J. Int. 179, 459–474. https://doi.org/10.1111/j.1365-246X.2009.04305.x.
Long, J., Shelhamer, E., Darrell, T., 2017. Fully convolutional networks for semantic segmentation. IEEE Trans. Pattern Anal. Mach. Intell. 39 (4), 640–651. https://doi.org/10.1109/TPAMI.2016.2572683.
Moczo, P., Kristek, J., Halada, L., 2000. 3D fourth-order staggered-grid finite-difference schemes: stability and grid dispersion. Bull. Seismol. Soc. Am. 90, 587–603. https://doi.org/10.1785/0119990119.
Ren, Z., Liu, Y., 2015. Acoustic and elastic modeling by optimal time-space domain staggered-grid finite-difference schemes. Geophysics 80 (1), T17–T40. https://doi.org/10.1190/geo2014-0269.1.
Ren, Z., Li, Z., 2017. Temporal high-order staggered-grid finite-difference schemes for elastic wave propagation. Geophysics 82 (5), T207–T224. https://doi.org/10.1190/geo2017-0005.1.
Robertsson, J.O.A., Blanch, J.O., Symes, W.W., 1994. Viscoelastic finite-difference modeling. Geophysics 59 (9), 1444–1456. https://doi.org/10.1190/1.1443701.
Siahkoohi, A., Louboutin, M., Herrmann, F.J., 2019a. Neural network augmented wave-equation simulation. arXiv preprint, arXiv:1910.00925vol. 2.
Siahkoohi, A., Louboutin, M., Herrmann, F.J., 2019b. The importance of transfer learning in seismic modeling and imaging. Geophysics 84 (6), A47–A52. https://doi.org/10.1190/GEO2019-0056.1.
Siahkoohi, A., Louboutin, M., Kumar, R., et al., 2018. Deep-convolutional neural networks in prestack seismic: two exploratory examples. In: 88th Annual International Meeting. SEG, Expanded Abstracts 2196–2200. https://doi.org/10.1190/segam2018-2998599.1.
Sobel, I., Feldman, G., 1968. A 3×3 isotropic gradient operator for image processing. In: Presented at the Stanford Artificial Intelligence Project, pp. 271–272.
Stork, C., 2013. Eliminating nearly all dispersion error from FD modeling and RTM with minimal cost increase. In: 75th Annual International Conference and Exhibition, EAGE. Extended Abstracts. https://doi.org/10.3997/2214-4609.20130478.
Virieux, J., 1984. SH-wave propagation in heterogeneous media: velocity-stress finite-difference method. Geophysics 49 (11), 1933–1957. https://doi.org/10.1190/1.1441605.
Wang, M., Xu, S., 2015. Finite-difference time dispersion transforms for wave propagation. Geophysics 80 (6), WD19–WD25. https://doi.org/10.1190/GEO2015-0059.1.
Wang, T.-C., Liu, M.-Y., Zhu, J.-Y., et al., 2018. High-resolution image synthesis and semantic manipulation with conditional GANs. arXiv preprint 2 arXiv:1711.11585.
Xu, T., Yan, H., Yu, H., et al., 2023. Removing time dispersion from elastic wave modeling with the pix2pix algorithm based on cGAN. Rem. Sens. 15 (12), 3120. https://doi.org/10.3390/rs15123120.
Yan, H., Xu, T., 2024. Suppressing spatial dispersion of seismic finite-difference modeling with the improved pix2pix algorithm. J. Comput. Phys. 511, 113129. https://doi.org/10.1016/j.jcp.2024.113129.
Yan, H., Yang, L., Li, X.-Y., 2016. Optimal staggered-grid finite-difference schemes by combining Taylor-series expansion and sampling approximation for wave equation modeling. J. Comput. Phys. 326, 913–930. https://doi.org/10.1016/j.jcp.2016.09.019.
Yang, D., Tong, P., Deng, X., 2012. A central difference method with low numerical dispersion for solving the scalar wave equation. Geophys. Prospect. 60, 885–905. https://doi.org/10.1111/j.1365-2478.2011.01033.x.
Yang, L., Yan, H., Liu, H., 2017. Optimal staggered-grid finite-difference schemes based on the minimax approximation method with the Remez algorithm. Geophysics 82 (1), T27–T42. https://doi.org/10.1190/GEO2016-0171.1.
Yao, G., Wu, D., Debens, H.A., 2016. Adaptive finite difference for seismic wavefield modelling in acoustic media. Sci. Rep. 6, 30302. https://doi.org/10.1038/srep30302.
Zhang, J., Yao, Z., 2013. Optimized finite-difference operator for broadband seismic wave modeling. Geophysics 78 (1), A13–A18. https://doi.org/10.1190/GEO2012-0277.1.
Zhang, Y., Cui, L., Song, L., et al., 2022. Numerical dispersion suppression based on joint deep learning in the space and wave number domains. Oil Geophys. Prospect. 57 (3), 510–524 (in Chinese). http://www.ogp-cn.com/CN/10.13810/j.cnki.issn.1000-7210.2022.03.002.